A Study on Mechanical Deformation of Highly Oriented Poly(oxymethylene) by Vibrational Spectroscopy and X-ray Diffraction: Stress and Temperature Dependences of Young's Modulus

Gang Wu, Kohji Tashiro, Masamichi Kobayashi,* Tamikuni Komatsu,† and Koichi Nakagawa‡

Department of Macromolecular Science, Faculty of Science, Osaka University, Toyonaka, Osaka 560, Japan. *Received March 3, 1988; Revised Manuscript Received July 20, 1988*

ABSTRACT: An effect of tensile stress on the Raman and infrared spectra of a highly oriented poly(oxymethylene) sample has been investigated at various temperatures in the range 20–160 °C. Among all the observed bands, the vibrational frequency of the skeletal modes was found to shift largely toward the lower side with increasing stress: $\Delta\tilde{\nu}/\Delta\sigma = -19$ cm^{-1}/GPa for the COC bending mode at 539 cm^{-1}, -15 cm^{-1}/GPa for the skeletal torsional mode at 231 cm^{-1}, and -6 cm^{-1}/GPa for the CO stretching mode at 920 cm^{-1}. As the temperature was raised, such a tendency became more remarkable. These spectroscopic results are consistent with the theoretically calculated molecular deformation mechanism, i.e., the mechanical strain energy concentrates on the internal displacement coordinates of the bending, torsional, and stretching modes of the skeletal chains. Such a deformation, intrinsic of the helical chain, is quite different from that of the planar zigzag polymers such as polydiacetylene and polyethylene, where the in-plane skeletal bending and stretching modes contribute mainly to the mechanical deformation. Based on the vibrational data, Young's modulus was evaluated as a function of stress and temperature by the lattice dynamical calculation. The calculated Young's modulus E_c^{calcd} is about 109 GPa for $\sigma = 0$ GPa and shows a negligibly small temperature dependence, different from the behavior of the "apparent" crystallite modulus E_c^{app} obtained by the X-ray diffraction measurement under the assumption of homogenous stress distribution within the sample. Based on the mechanical complexed model presented by Ward et al., the "true" crystallite modulus E_c^{true} was estimated from E_c^{app}. It is about 100 GPa at −150 °C and close to the spectroscopically estimated value of 109 GPa. E_c^{true} decreases drastically above −100 °C and is about 75 GPa at 20 °C. The difference between E_c^{calcd} and E_c^{true} in the high-temperature region may be ascribed to the decrease in modulus due to an occurrence of the large-amplitude molecular motion.

Introduction

When a polymer crystal is mechanically deformed, the atomic arrangement is forced to change so that the energetical increment of the system is minimized.[1] The lattice dynamical theory predicts such a mechanical deformation mechanism at the atomic level. The most direct and powerful way to prove such a prediction experimentally may be a utilization of a vibrational spectroscopic method under an external mechanical condition, because it is very sensitive to the local changes in the internal coordinates such as bond length, bond angle, and internal rotation. In the present paper we will focus our attention only to the case of the tensile force applied along the chain axis.

The measurement of infrared absorption spectra under tension has been reported for several kinds of crystalline polymers, the results being interpreted based on the concept of anharmonic vibration.[2-7] But most of these studies have not been developed so as to predict the anharmonicity or the stress and temperature dependence of the mechanical property such as Young's modulus of the polymer chain.

As a trial to grasp a concrete relationship between Young's modulus and the molecular deformation mechanism of a polymer, we measured the resonance Raman spectra of a polydiacetylene (PDA) single crystal under the application of external tensile force.[8] This polymer can be obtained in the form of a giant single crystal and so the problem of the assumption of a homogeneous stress distribution may not be necessary to take into consideration. The Raman bands intrinsic of the skeletal deformation mode (stretching and bending modes of C=C and C≡C linkages) were found to shift to the lower frequency side, as reported first by Mitra and Batchelder.[9,10] In addition to it, we succeeded in observing the low-frequency shift of the stretching mode of the C—C single bond by the polarized FTIR measurement for PDA single crystal under tension.[11] Such a spectral change is consistent with the calculated atomic displacements of a polydiacetylene chain induced by the tensile stress: the atoms are displaced so that the strain energy concentrates on the stretching and bending coordinates of skeletal chain. Based on thus obtained vibrational data, we calculated Young's modulus of the polydiacetylene chain, which was found to decrease with a rate of 0.7 GPa for a 1 GPa increment of tensile stress. Such a tendency of decrement became remarkable with increasing temperature, consistent qualitatively with the observed stress/temperature dependence of the bulk Young's modulus of a polydiacetylene giant single crystal. Quantitatively, however, the theoretical calculation could not reproduce the observed behavior of Young's modulus. One of the reasons for such a discrepancy may come from the lack of information concerning a contribution of the internal rotational modes, which will displace the atoms out of the zigzag plane and so reduce the modulus at a finite temperature. But the data concerning such an internal rotational mode are difficult to obtain because of the symmetry limitation for the optical activity for the planar zigzag conformation. Thus the dependence of Young's modulus on stress and/or temperature has not yet been discussed enough on the basis of a full set of vibrational data including this additional information.

Then, as the second trial, we have searched for a polymer system that can give us more fruitful information so as to discuss the anharmonic behavior of Young's modulus. We selected poly(oxymethylene) (POM) as a candidate, which has the simplest helical structure and provides a variety

† Asahi Chemical Industry Co. Ltd., Fuji, Shizuoka 416, Japan.
‡ NTT Electrical Communications, Tokai, Ibaraki 319-11, Japan.

0024-9297/89/2222-0758$01.50/0

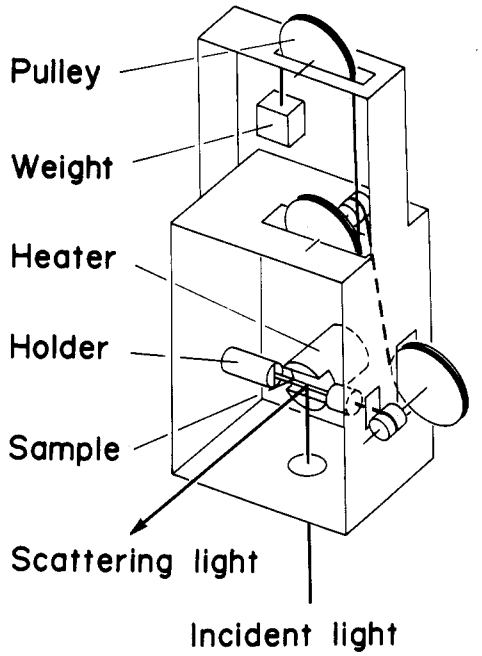

Figure 1. Schematic diagram of the Raman spectral measuring system under stress.

of vibrational modes including bond stretching, bond angle deformation, and internal rotations of the skeletal chain. A great amount of the vibrational spectroscopic data accumulated so far will be an important and useful basis for proceeding with the present study.[12-15]

The usually drawn POM samples are opaque with many voids. These opaque samples are not suitable for the optical scattering experiments and not strong enough for mechanical deformation. Recently many trials have been made to produce the ultradrawn POM samples.[16-18] The so-called "pressurized drawing" method can produce successfully the highly oriented and highly transparent POM samples with a high Young's modulus.[18] In the present paper, using this transparent POM sample, the measurement of the polarized Raman spectra and the infrared absorption spectra was made under the externally applied stress at various temperatures. The results were analyzed by the normal coordinates treatment: the determined force field was utilized to estimate the stress and temperature dependence of Young's modulus. Thus theoretically predicted anharmonic behavior of the modulus was actually compared with the crystallite modulus measured by the X-ray diffraction method. The molecular deformation mechanism of a helical chain is predicted to be much different from the case of a planar zigzag chain. The vibrational spectroscopic data will be also used to discuss such a difference in the deformation mechanism among poly(oxymethylene), polydiacetylene, and polyethylene.

Experimental Section

Samples. For the Raman spectral measurements under tension, two kinds of POM samples were utilized: (1) a sample prepared by the so-called pressurized drawing method (the draw ratio 17, bulk Young's modulus 36 GPa) and (2) a sample prepared by the dielectric heating method (the draw ratio 34, bulk modulus 58 GPa). The optical transparency is good for the sample (1). Thus, the experimental results on the sample (1) will be mainly described in this paper, although the essential feature of the data is not so different from that of the sample (2).

For the far-infrared spectral measurement, the oriented POM films prepared by stretching the melt-quenched samples (Delrin 100) to about 6.5 times the original length followed by a heat treatment at 165 °C under tension were used. The film thickness was about 50 μm.

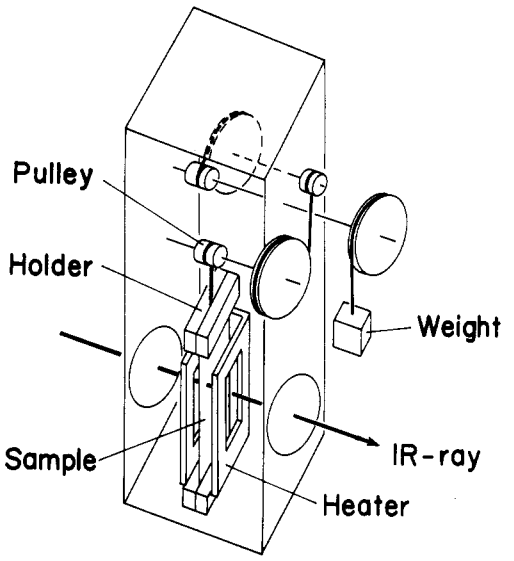

Figure 2. Schematic diagram of the infrared spectral measuring system under stress.

Raman and Far-Infrared Measurements under Tension. For the Raman spectral measurements under tension at various temperatures, a loading system shown in Figure 1 was designed and utilized. The rod sample was set horizontally. One end of the sample was fixed at the holder and the other end was tensioned by applying a weight through a pulley set, which enlarges the stress working on the sample by a principle of bar. The stress was calculated from the applied weight divided by the cross-sectional area of the sample. The sample was heated with a flexible heater surrounding it. The temperature was monitored by a CA thermocouple and controlled within ±1–2 °C. The polarized Raman spectra were measured with a 90° scattering geometry. The 514.5-nm emission line from an Argon ion laser was used as an excitation light. The Raman spectra were taken with a Japan Spectroscopic Co. NR 1000 Raman spectrophotometer. In order to increase the measurement accuracy of the wavenumber, the natural emission lines from the Ar ion laser were utilized as the standard.

The stress dependence of the far-infrared absorption spectra was measured by using an optical cell shown in Figure 2. The POM film was set vertically and tensioned into the upward direction. The far-infrared spectra were recorded at various temperatures by a Hitachi FIS-3 far-infrared spectrophotometer.

Measurement of Stress–Strain Curves of the Crystalline Region. The stress–strain curves of the POM crystalline phase were measured by an X-ray diffraction method. The stretching device was transferred from that used in the Raman scattering measurement (Figure 1) with some modification. Nickel-filtered Cu Kα (λ = 1.5418 Å) radiation was utilized as an incident X-ray source. The stress dependence of the meridional (009) reflection was measured by a θ–2θ scanning method using an X-ray photocounter. Characteristic diffraction lines from an aluminium powder were used as a standard for the 2θ angle.

Results and Discussion

Stress Dependence of the Polarized Raman Spectra. Figure 3 shows the polarized Raman spectra of POM measured under free tension at room temperature. Polarization measurement could be made successfully by using the transparent POM sample produced by the pressurized drawing method. The Raman bands observed in Figure 3 can be assigned to the A_1, E_1, and E_2 symmetry species.[15] Referring to the normal mode analysis, the bands at 539 (A_1), 635 (E_1), 920 (A_1), 937 (E_1), and 1095 cm^{-1} (E_1) were assigned to the vibrational modes of δ(COC), δ(OCO), ν_s(COC), ν_s(COC), and ν_a(COC), respectively.[15] Here δ denotes the bending mode of the bond angle and ν the bond stretching mode. The subscripts "s" and "a" denote the symmetric and antisymmetric vibrational modes, re-

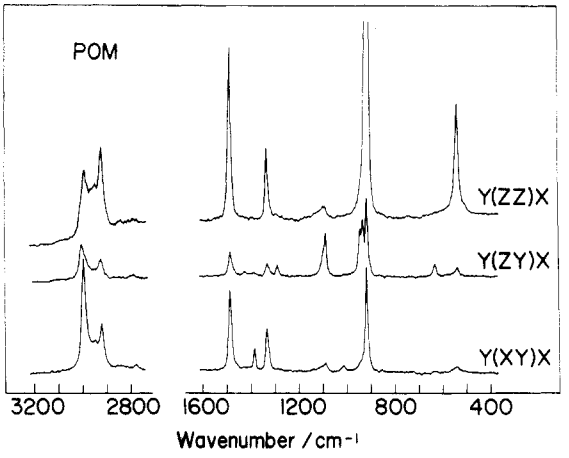

Figure 3. Polarized Raman spectra of POM sample (z is parallel to the chain axis).

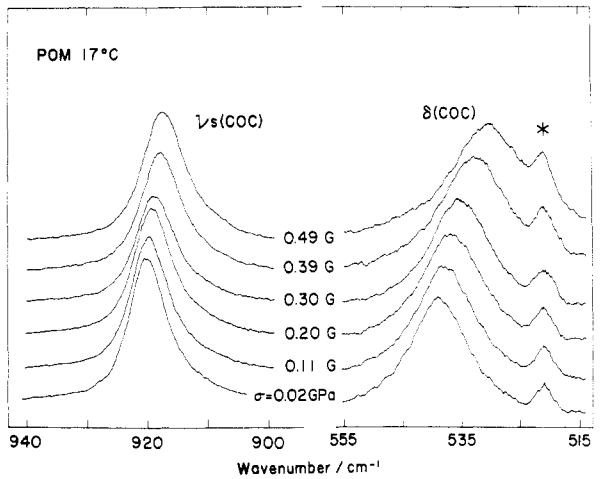

Figure 4. Stress dependence of the Raman spectra measured for the δ(COC) and ν_s(COC) bands of POM at 17 °C. The peak at 521 cm^{-1} is due to the emission from Ar$^+$ laser.

spectively. The bands located in the frequency region higher than 1200 cm^{-1} were assigned to such local vibrational modes as twisting, wagging, and stretching modes of the methylene side group.

Figure 4 shows the stress-induced Raman spectral changes measured for the skeletal vibrational modes at 539 cm^{-1} [A_1, δ(COC)] and 920 cm^{-1} [A_1, ν_s(COC)] at room temperature. A 521-cm^{-1} peak is a natural emission from Argon ion laser utilized as a wavenumber standard. As the stress increases, the peak position of the bands is found to shift to the lower frequency side. Similar measurements were also made to the other Raman-active bands observed in Figure 3. In Figure 5 is shown the change in the infrared-active skeletal torsional mode at 231 cm^{-1} [A_2, τ(CO)] under tension at room temperature.

Figure 6 shows the stress dependence of the vibrational frequencies of the bands observed in the Raman and far-infrared spectra of Figures 3–5 at room temperature. Among all the observed bands, the vibrational frequencies related to the skeletal deformation modes, i.e., ν_a(COC), ν_s(COC), δ(COC), and τ(CO), are found to decrease largely by the application of tensile stress. In particular, the shifts in δ(COC) and τ(CO) modes are remarkable: the slopes are $\Delta\tilde{\nu}/\Delta\sigma$ = −19 cm^{-1}/GPa and −15 cm^{-1}/GPa, respectively. The shifts of ν_s(COC) and ν_a(COC) modes are about −6 cm^{-1}/GPa. The wavenumber changes of the local methylene modes were too small to detect with high enough accuracy in the stress range 0–0.5 GPa. The vibrational bands at 39 cm^{-1} (E_1) and 65 cm^{-1} (E_2) show a high-frequency shift under tension. These bands may be coupling modes between the skeletal torsional mode and the vibrational lattice mode.[19] The tension along the chain

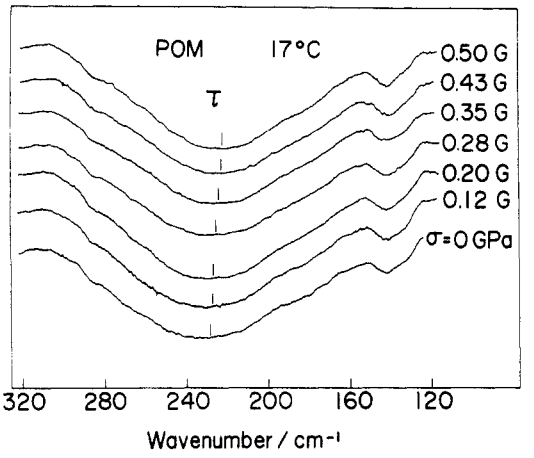

Figure 5. Stress dependence of the infrared spectra measured for the skeletal torsional band τ(CO) of POM at 17 °C.

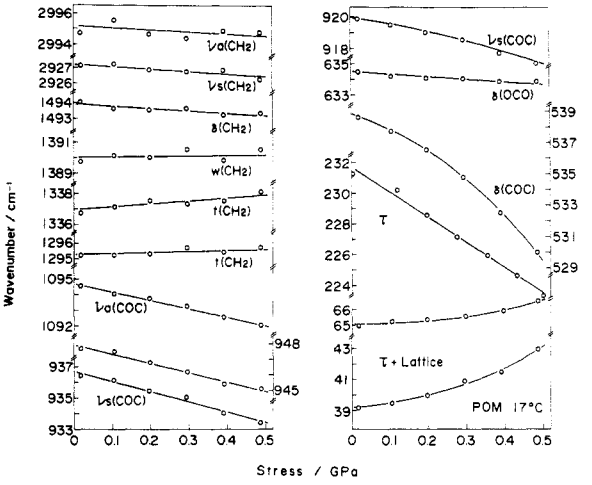

Figure 6. Stress dependence of vibrational frequencies for some observed bands of POM at 17 °C.

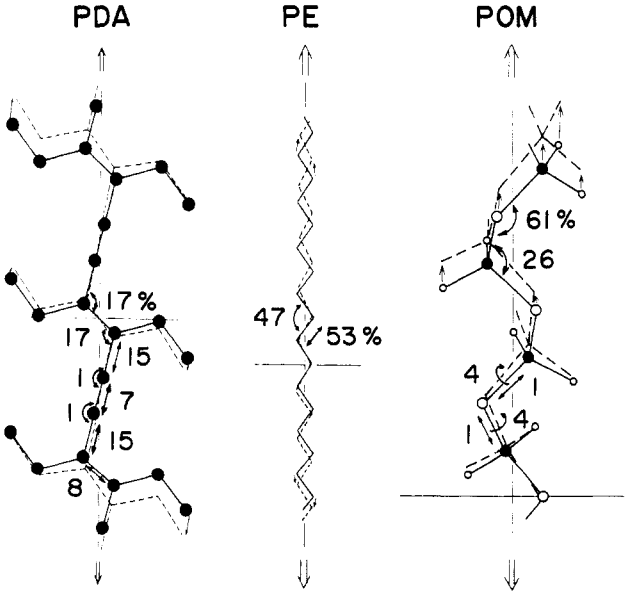

Figure 7. Atomic displacements and the potential energy distribution calculated for POM helical chain, polyethylene (PE) and polydiacetylene (PDA) under the hypothetically large tensile strain of 10%. The solid and broken lines represent the undeformed and deformed conformations of the chain, respectively.

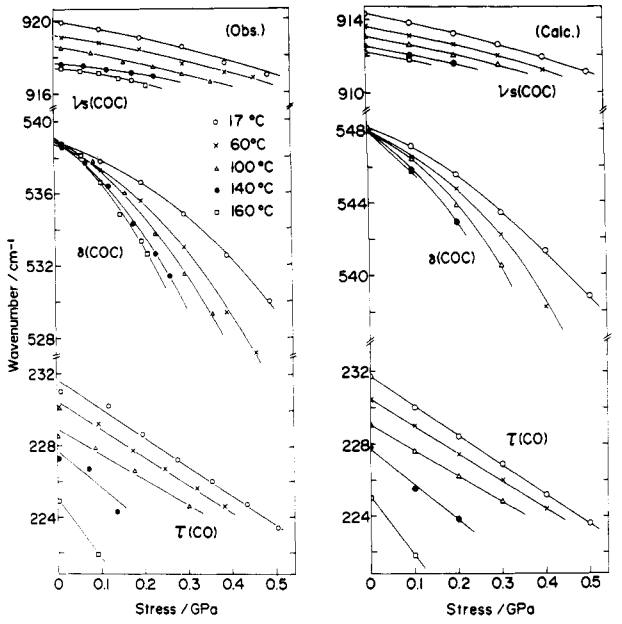

Figure 8. Comparison between the observed and calculated stress dependence of the vibrational frequencies for the ν_s(COC), δ(COC), and τ(CO) bands of POM at the various temperatures.

axis may cause the lateral shrinkage due to Poisson's effect which increases the intermolecular interaction, resulting in the high-frequency shift of these bands.

Figure 7 shows the atomic displacements and potential energy distribution (PED) calculated for a POM (9/5) helical chain under the tensile strain of 10% in comparison with those for polyethylene[1] and polydiacetylene. The details of parameters used in calculation will be described in a later section. For POM, the PED concentrates mainly on the skeletal bending modes [δ(COC) and δ(OCO)], the skeletal torsional mode τ(CO), and the CO stretching mode ν(COC). This is quite consistent with the spectroscopic results measured under stress as shown in Figure 6. In the case of planar zigzag conformation of polydiacetylene and polyethylene, in contrast, the PED concentrates mainly on the bond stretching and bond-angle deformation modes of the skeletal chains in almost equal percentages. These theoretical predictions were also proved experimentally by the Raman and infrared spectral measurements under tension.[7,8,11,20]

Stress and Temperature Dependences of the Intramolecular Force Field. Figure 8 shows the stress-induced vibrational frequency shift measured at various temperatures for three types of skeletal modes: ν_s(COC), δ(COC), and τ(CO). It can be noticed here that the frequency shift becomes larger as the temperature is raised. Using these spectral data, the intramolecular force constants were determined as a function of stress and temperature by the normal mode treatment so that the calculated wavenumbers gave a good reproducibility for the observed vibrational frequencies. The molecular structure parameters used in the calculation are as follows: bond lengths r_{C-O} = 0.142 nm and r_{C-H} = 0.109 nm; bond angles $\angle$COC = 112.4°, $\angle$OCO = 110.8°, $\angle$HCH = 109.5°, and $\angle$HCO = 109.1°; and internal-rotation angles τ(CO) = 78.2°.[12] As the initial set of the force constants, we employed that reported by Tadokoro et al. (the Urey-Bradley type, set 17).[12] The normal mode calculation was made according to the GF matrix method.[21] A comparison between the calculated and observed stress dependence of the vibrational frequencies of ν_s(COC), δ(COC), and τ(CO) modes is made in Figure 8. A fairly good agreement was obtained between them. In the normal mode calculation

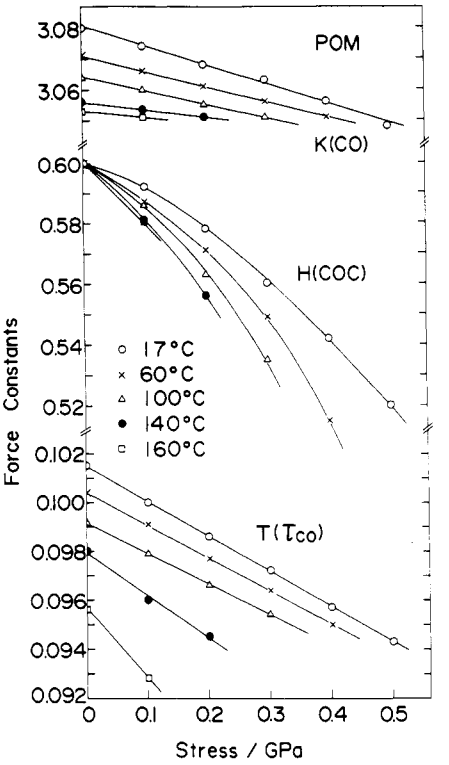

Figure 9. Stress dependence of intramolecular force constants for a POM single chain at the various temperatures. The units are 10^2 N m^{-1} for K(CO), 10^2 Nm rad^{-2} for H(COC), and 10^2 N m^{-1} for $T(\tau_{CO})$.

only three types of force constants K(CO), H(COC), and $T(\tau_{CO})$ were modified, which relate with the skeletal modes of chain. The force constants relating with the CH_2 side groups [K(CH), H(HCO), and H(HCH)] were fixed in the approximation because the vibrational modes localized in such side groups did not show any frequency shift within the experimental error as seen in Figure 6. Figure 9 shows the stress dependence of the force constants K(CO), H(COC), and $T(\tau_{CO})$ at various temperatures. These force constants soften gradually with an increment of stress and temperature. For example, the decrease in K(CO), H(COC), and $T(\tau_{CO})$ is about 2%, 27%, and 14%, respectively, for the application of tensile stress of 1 GPa at room temperature.

Stress and Temperature Dependences of Young's Modulus. Using thus obtained force constants, the theoretical Young's modulus of POM chain E_c^{calcd} was calculated as a function of stress and temperature. The molecular chain is deformed under tension and the atomic position as well as the force field may be modified by the externally applied force. The chain conformation tends to stretch toward the planar zigzag form although the deformation is infinitesimally small, and so the geometrical change may increase the modulus to some extent. But the actually observed crystallite modulus decreases with tension (see Figure 13), indicating that such a geometrical factor might not be so large compared with the influence of the force-field change due to the anharmonicity. In the present calculation, therefore, the geometrical factor was neglected in the first approximation, i.e., the atomic positions were assumed to be the same as those under free tension. Such a neglection of the geometrical factor is considered to appear in the form of an overestimation of the force constant change under tension. The calculation was based on the lattice dynamic theory described in ref 22. In Figure 10, the calculated Young's modulus is plotted against stress. The calculated value under free tension is

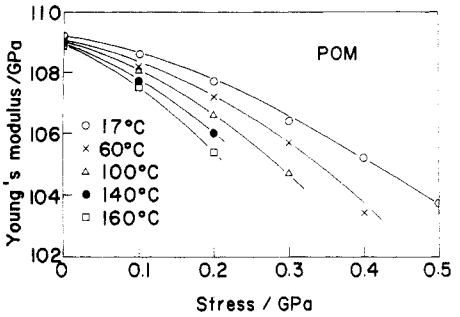

Figure 10. Stress dependence of Young's modulus calculated for a POM chain at the various temperatures.

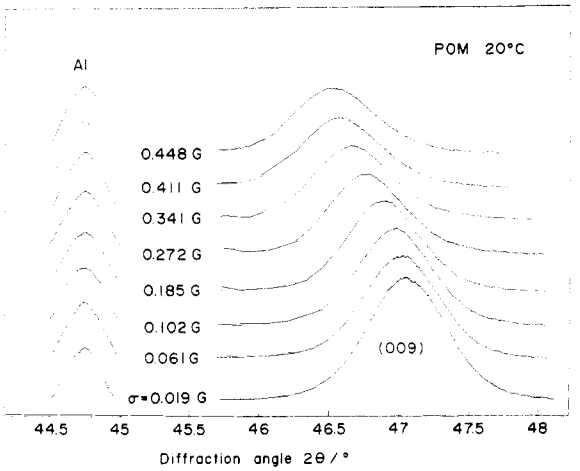

Figure 11. Stress dependence of the X-ray (009) reflection for POM at 20 °C. The reflectional peak at about 44.7° is from an aluminium powder.

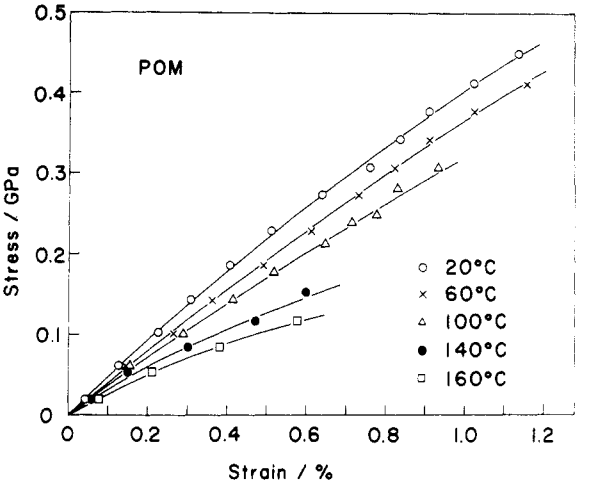

Figure 12. Stress–strain curves measured by the X-ray diffraction for POM in the temperature range 20–160 °C.

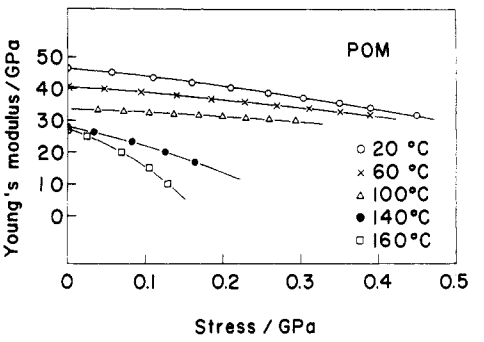

Figure 13. Stress dependence of Young's modulus E_c^{app} measured in the temperature range 20–160 °C.

109.2 GPa at room temperature. The modulus decreases as the applied stress is increased. Such a tendency becomes more remarkable at higher temperature.

In order to check out the reasonableness of the calculated Young's modulus, we have measured the crystallite modulus as a function of stress and temperature by X-ray diffraction method. The temperature dependence of crystallite modulus of POM has been already reported by several workers.[23-25] According to Ward et al.,[24] the crystallite modulus and its temperature dependence are not necessarily independent of the preparation history of the sample, although the variation might not be so remarkable. Therefore, we measured the crystallite modulus for the sample just utilized in the present Raman spectral measurements. Figure 11 illustrates an angular shift of meridional (009) reflection induced by a tensile stress at room temperature. A reflection at 44.7° is from an aluminium powder used as a standard for the diffractional angle. In Figure 12 are summarized the stress and strain curves measured for the POM crystalline region along the chain axis at various temperatures. Differentiation of the curve with respect to the strain or $(\partial\sigma/\partial\epsilon)_{\sigma,T}$ gives an "apparent" crystallite modulus E_c^{app} at each stress and temperature. The term "apparent" is added, as proposed by Ward et al., because the stress applied onto the crystalline region is assumed to be equal to the bulk stress. In Figure 13 is plotted the stress dependence of thus obtained E_c^{app} at various temperatures. The crystallite modulus decreases with an increment of stress and/or temperature: this tendency is qualitatively consistent with the theoretical results shown in Figure 10. Quantitatively, however, the observed modulus is much smaller than E_c^{calc} under the same stress and temperature conditions: for example, under free tension, the observed E_c^{app} is about 47 GPa, while the E_c^{calcd} is 109 GPa. The calculated modulus is almost constant in the temperature range 17–160 °C, while the observed modulus decreases by about 43%. When the tensile stress is increased from 0 to 0.5 GPa at room temperature, the calculated decrease in modulus is only 5%, while the observed decrement is about 34%. As the temperature is increased, the difference between the calculated and observed changes in modulus becomes more remarkable.

Estimation of the Temperature Dependence of True Crystallite Modulus. In the above paragraph, we pointed out a large difference in the behavior of the spectroscopically estimated and the X-ray observed moduli. Before discussing the reason for it, we must first eliminate the superfluous factor affecting apparently the crystallite modulus measured by the X-ray diffraction method, that is, an assumption of the uniform stress distribution. On the basis of the experimental results on E_c^{app} measured in the temperature region of −150 to 20 °C, Ward et al. pointed out that the assumption of the series model (the crystallite stress equals to the bulk stress) is not applicable at least for the POM case.[24] They analyzed the temperature dependence of E_c^{app} on the basis of the complexed mechanical model or the Takayanagi model and estimated the "true" crystallite modulus E_c^{true} of POM. In order to estimate the temperature dependence of E_c^{true} in the whole range −150 to 160 °C on the basis of all the data reported so far, their method of calculation is transferred here. As shown in Figure 14, in the parallel-series model, the material is regarded as a mechanical system composed of the crystal (b)–amorphous ($1 - b$) parallel fraction (a) coupled in series with the crystalline part ($1 - a$). [The "series-parallel" model must be also considered here, which is composed of the parallel arrangement of the crystal

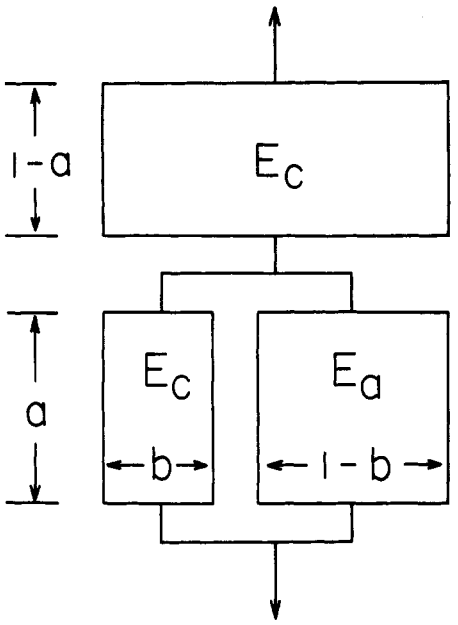

Figure 14. Schematic representation of the parallel-series model.

phase (b) and the amorphous (a)–crystalline ($1-a$) series phase ($1-b$). But the calculated results are not so deviated from those for the "parallel-series" model.] According to this parallel-series model, E_c^{app} and the bulk modulus E_b are expressed in the following equations.

$$E_c^{app} = xE_c^{true}\left[1 - a + \frac{ab}{b + (1-b)E_a/E_c^{true}}\right]^{-1} \quad (1)$$

$$E_b = \left[\frac{1-a}{E_c^{true}} + \frac{a}{bE_c^{true} + (1-b)E_a}\right]^{-1} \quad (2)$$

where E_a and E_c^{true} are the moduli of the amorphous and crystalline phases, respectively. The degree of crystallinity x is given by

$$x = 1 - a + ab \quad (3)$$

The details of the calculating process are not described here,[26] but only the outlines are mentioned. By choosing suitable values of the parameters x, a, and b as a function of the drawing ratio of the sample and Young's modulus of the amorphous phase E_a,[26] we can reproduce systematically and consistently all the data of E_c^{app} and E_b from ref 23–25 and the present study. The most plausible value of E_c^{true} was estimated as about 75 GPa at room temperature. [In Figure 15 is shown the comparison between the observed and calculated moduli, where the straight 45° line indicates a complete coincidence between the calculated and observed values. As seen here, E_c^{true} = 75 GPa (± 10GPa) can give a satisfactory result within the experimental error, while the utilization of the theoretical value 109 GPa as E_c^{true} gives too high calculated values of E_c^{app}.] The fact that the all reported data of E_c^{app} and E_b can be simulated satisfactorily suggests a reasonableness of the parallel-series model utilized here.

At the next stage, then, we try to estimate the temperature dependence of E_c^{true} on the basis of the same process as for the room temperature data. But the utilizable experimental data of E_c^{app} and E_b at low- and high-temperature regions are very limited and so we cannot carry out the optimization of the E_c^{true} by such a treatment. As pointed out above, we have now a set of the numerical parameters a, b, and x for the POM samples with various drawing ratios.[26] Then by assuming that these values are not dependent on temperature and also by assuming a suitable temperature change in E_a, which does not affect the final result so seriously as clarified previously,[26] the E_c^{true} was obtained by solving eq 1 based on the reported E_c^{app} values, where the data are from Ward et al.[24] and Nakamae et al.[25] in the range −150 to 20 °C and from Figure 13 in the range of 20–160 °C. Thus obtained E_c^{true} were plotted against temperature in Figure 16b. The E_c^{true} exhibits an appreciably large temperature dependence: E_c^{true} is about 100 GPa below −120 °C, decreases down to about 80 GPa at room temperature, and furthermore decreases to 40–50 GPa at higher temperatures. Contrary to it, the theoretical modulus calculated based on the vibrational spectroscopic data, about 109 GPa, shows almost no temperature dependence in the temperature region −150 to 160 °C. The value is rather close to the E_c^{true} value estimated at a low temperature of −150 °C.

As a possible reason for such a discrepancy, there may exist a problem of time scale in the measurement of the modulus. The X-ray diffraction method is static, while the vibrational data are for the frequency region of 10^{12} s^{-1}. That is to say, the former is in the isothermal condition, whereas the latter is in the adiabatic condition. The moduli for these two conditions are approximately related with each other as[27]

$$\frac{1}{E_{ad}} \doteq \frac{1}{E_{iso}} - \alpha_l^2 \frac{T}{\rho C_v} \quad (4)$$

where E_{ad} and E_{iso} are the moduli for the adiabatic and isothermal conditions, respectively. α_l is a thermal expansion coefficient along the chain axis, ρ is a density, and C_v is a specific heat. In the case of POM, $\alpha_l \doteq -0.5 \times 10^{-6}$

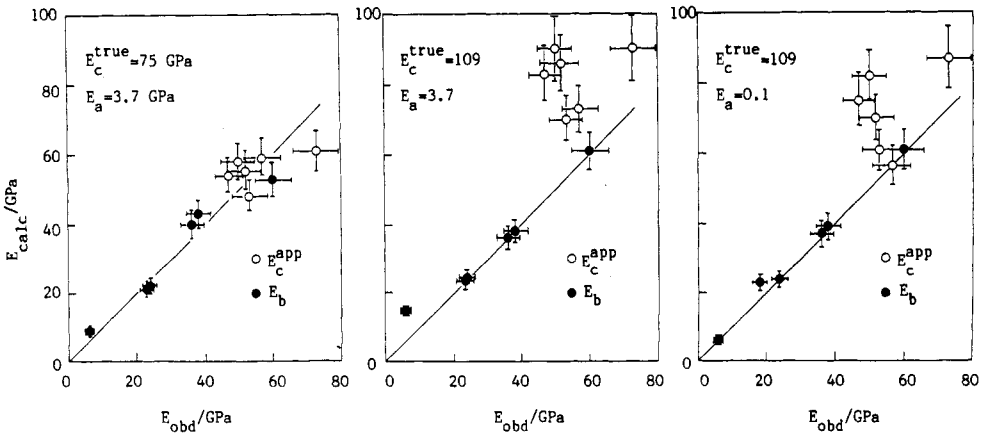

Figure 15. Comparison between the calculated and observed Young's moduli of E_c^{app} and E_b for the various E_c^{true} and E_a based on the parallel-series model (room temperature).

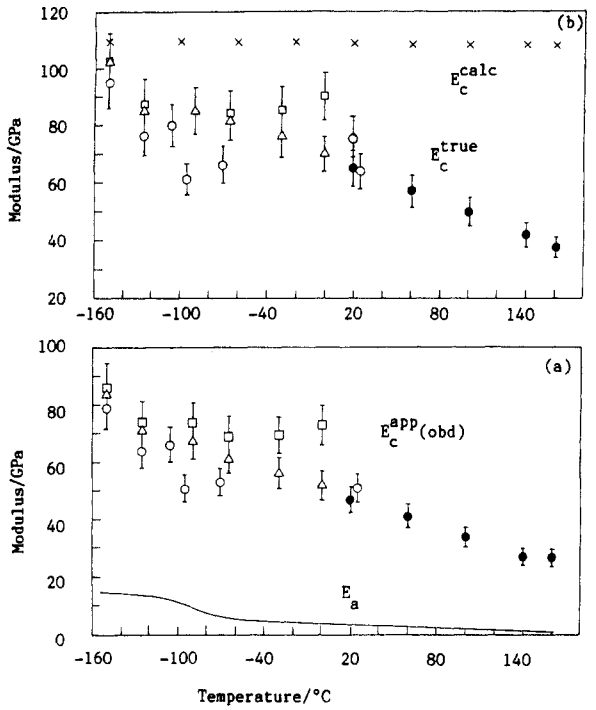

Figure 16. (a) Temperature dependence of the observed E_c^{app} and the assumed E_a. The data of E_c^{app} are from ref 23, 24, and 25 and the present study. (b) Temperature dependence of E_c^{true} estimated from the observed E_c^{app} (a). Cross points indicate the spectroscopically calculated values of E_c^{calc}.

K^{-1}, ρ = 1.49 g/cm^3, and C_v ≒ 0.35 cal/(g K) at room temperature.[25,28,29] Then, at T = 300 K

$$E_{ad} - E_{iso} \fallingdotseq (E_{iso})^2 \frac{\alpha_l^2 T}{\rho C_v} \fallingdotseq 2 \times 10^{-4} \text{ GPa} \qquad (5)$$

which is negligibly small to explain the above-mentioned difference in the modulus, 109 and 75 GPa. Thus the difference in the time scale for the measurement of the modulus may not be needed to consider at least for the crystalline region.

The spectroscopically calculated modulus is considered as a limiting modulus expected to appear at the absolute temperature 0 K, because the calculation takes into account only the static potential field and any thermally activated large-amplitude molecular motions are not included. Chiba et al.[30] clarified that the POM molecular chains experience a thermal motion due to the large-amplitude torsional modes around C–O skeletal bonds, which begins to occur above −100 °C. Below it, the lattice is in the standing state with rigid and regular chains. The temperature dependence of the E_c^{true} seen in Figure 16b corresponds well to the curve for the second moment of the broad-line NMR spectra.[30] Occurrence of the rotational fluctuation at room temperature in trigonal POM has been detected by the disappearance of the 100-cm^{-1} far-infrared band of the rotational lattice mode.[31] That is to say, the theoretically calculated modulus E_c^{calcd}, without any consideration of thermally activated large-amplitude molecular motions, is considered to correspond to the E_c^{true} at an extremely low temperature (<−150 °C). The E_c^{true} begins to decrease largely in the vicinity of the temperature where the large-amplitude internal rotations start to occur.

Conclusions

In the present paper we discussed mainly the following three items.

(1) The Raman and infrared spectra of highly oriented transparent POM sample were measured under tension, and the skeletal vibrational modes were found to show an appreciably large frequency shift. These experimental results are quite consistent with the theoretically predicted molecular deformation mechanism of a POM helical chain.

(2) On the basis of lattice dynamics, the vibrational frequencies and Young's modulus were calculated as a function of stress and temperature. The calculated Young's modulus is about 109 GPa and shows a small decrease with increasing stress and temperature.

(3) The X-ray observed crystallite modulus was found to show a much larger stress/temperature dependence compared with the spectroscopically calculated result. Then, utilizing the complexed mechanical model proposed by Ward et al., the "true" crystallite modulus E_c^{true} was estimated from the X-ray data in the temperature region of −150 to 160 °C. The E_c^{true} at low temperature, 100 GPa, was found to agree well with the calculated modulus, 109 GPa. As the temperature increases, the E_c^{true} is found to decrease largely. It is possibly because of an occurrence of thermally activated molecular motion of the POM chain, as supported by the X-ray and NMR studies.

Acknowledgment. We are grateful to Dr. Masahiro Setoguchi of the Government Industrial Research Institute, Osaka, Japan, for giving us a chance to use an X-ray photocounter system. This work was supported in part by a Grand-in-Aid on Scientific Research on Priority Areas, New Functionality Materials—Design, Preparation and Control, The Ministry of Education, Science and Culture, Japan.

Registry No. POM, 9002-81-7; Delrin 100, 94947-58-7.

References and Notes

(1) Tashiro, K.; Kobayashi, M.; Tadokoro, H. *Macromolecules* **1977**, *10*, 413.
(2) Roylance, D. K.; DeVries, K. L. *Polym. Lett.* **1971**, *9*, 443.
(3) Vettegren, V. I.; Novak, I. I. *J. Polym. Sci., Polym. Phys. Ed.* **1973**, *11*, 2135.
(4) Voroboyev, V. M.; Razumovskaya, I. V.; Vettegren, V. I. *Polymer* **1978**, *19*, 1267.
(5) Wool, R. P.; Boyd, R. H. *J. Appl. Phys.* **1980**, *51*, 5116.
(6) Bretzlaff, R. S.; Wool, R. P. *Macromolecules* **1983**, *16*, 1907.
(7) Wool, R. P.; Bretzlaff, R. S.; Li, B. Y.; Wang, C. H.; Boyd, R. H. *J. Polym. Sci., Polym. Phys. Ed.* **1986**, *24*, 1039.
(8) Wu, G.; Tashiro, K.; Kobayashi, M. *Rep. Prog. Polym. Phys. Jpn.* **1987**, *30*, 127.
(9) Mitra, V. K.; Risen, W.; Baughman, R. H. *J. Chem. Phys.* **1977**, *66*, 2731.
(10) Batchelder, D. N.; Bloor, D. *J. Polym. Sci., Polym. Phys. Ed.* **1977**, *17*, 569.
(11) Wu, G.; Tashiro, K.; Kobayashi, M. *Macromolecules*, in press.
(12) Tadokoro, H.; Kobayashi, M.; Kawaguchi, Y.; Kobayashi, A.; Murahashi, S. *J. Chem. Phys.* **1963**, *38*, 703.
(13) Zamboni, V.; Zerbi, G. *J. Polym. Sci.* **1964**, *7*, 153.
(14) Sugeta, H.; Miyazawa, T. *Polym. Lett.* **1969**, *7*, 251.
(15) Morishita, H.; Kobayashi, M. *Rep. Prog. Polym. Phys. Jpn.* **1987**, *30*, 131.
(16) Brew, B.; Ward, I. M. *Polymer* **1978**, *19*, 1338.
(17) Nakagawa, K.; Konaka, T.; Yamakawa, S. *Polymer* **1985**, *26*, 84.
(18) Komatsu, T.; Enoki, S.; Aoshima, A. *Polym. Prepr. Jpn.* **1986**, *35*, 3712.
(19) Sugeta, H. Ph.D. Thesis, Osaka University, 1969.
(20) Wu, G.; Tashiro, K.; Kobayashi, M. *Rep. Prog. Polym. Phys. Jpn.* **1987**, *30*, 143.
(21) Tadokoro, H. *Structure of Crystalline Polymers*; Wiley Interscience: New York, 1979.
(22) Tashiro, K.; Kobayashi, M.; Tadokoro, H. *Macromolecules* **1977**, *10*, 731.
(23) Sakurada, I.; Ito, T.; Nakamae, K. *J. Polym. Sci., Part C* **1966**, *15*, 75.
(24) Jungnitz, S.; Jakeways, R.; Ward, I. M. *Polymer* **1986**, *27*, 1651.
(25) Nakamae, K.; Nishino, T.; Shimizu, Y.; Hata, K.; Matsumoto, T. *Polym. Prepr. Jpn.* **1987**, *36*, 2438.
(26) Tashiro, K.; Wu, G.; Kobayashi, M. *Polymer* **1987**, *29*, 1768.
(27) Mason, W. P. *Piezoelectric Crystals and Their Application to Ultrasonics*; Van Nostrand: Princeton, NJ, 1950.

(28) White, G. K.; Smith, T. F.; Birch, J. A. *J. Chem. Phys.* **1976**, *65*, 554.
(29) Dainton, F. S.; Evans, D. M.; Hoare, F. E.; Melia, T. P. *Polymer* **1962**, *3*, 263.
(30) Chiba, A.; Hasegawa, A.; Hikichi, K.; Furuichi, J. *J. Phys. Soc. Jpn.* **1966**, *21*, 1777.
(31) Kobayashi, M.; Morishita, H.; Shimomura, M.; Iguchi, M. *Macromolecules* **1987**, *20*, 2453.

Structural Reorganization of Phosphatidylcholine Vesicle Membranes by Poly(2-ethylacrylic acid). Influence of the Molecular Weight of the Polymer

Ulrich K. O. Schroeder and David A. Tirrell*

Department of Polymer Science and Engineering, University of Massachusetts, Amherst, Massachusetts 01003. *Received March 22, 1988; Revised Manuscript Received March 25, 1988*

ABSTRACT: Three samples of poly(2-ethylacrylic acid) (PEAA) of different molecular weights ($\bar{M}_w$ = 164 000, 43 000, and 12 000) were prepared by radical polymerization of 2-ethylacrylic acid in bulk. The conformational properties of the samples were determined and correlated with the pH-dependent structural reorganization observed in phosphatidylcholine vesicles suspended in the respective polymer solutions. In all experiments the sample of lowest molecular weight behaved differently from the other two: The cooperativity of the conformational transition was reduced and the transition midpoint was shifted to lower pH as compared to the samples of higher molecular weight. These effects of polymer molecular weight were reflected in the behavior of the vesicle-to-micelle transition observed upon acidification of aqueous mixtures of PEAA and dipalmitoylphosphatidylcholine.

Introduction

The pH-dependent conformational transition of poly(2-ethylacrylic acid) (PEAA, **1**) has been used to sensitize

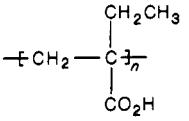

1

synthetic bilayer membranes to changes in pH,[1] temperature,[2] light intensity,[3] and solute (e.g., glucose) concentration.[4] The mechanism of the membrane response has been shown to consist of a structural reorganization of the membrane lipid from a vesicular form at high pH to a mixed polymer–lipid micelle at low pH, the reorganization being driven by collapse of the polymer chain from an extended, hydrophilic form to a compact, hydrophobic coil upon acidification.[5]

The use of macromolecules to effect molecular switching in synthetic bilayer membranes offers substantial advantages in membrane design. One would anticipate, for example, that the pH-dependent conformational transition of PEAA[6-8] would be subject to modulation by variation in polymer chain structure (e.g., in tacticity or molecular weight) and that one might exploit such variations to adjust either the "critical" pH for membrane regorganization[1] or the cooperativity of the structural transition.

In our previous work on the interaction of PEAA with dipalmitoylphosphatidylcholine (DPPC, **2**), we prepared

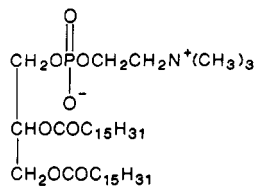

2

polymer samples that spanned a range of tacticities from 91% isotactic triads to 88% syndiotactic triads, and we found that there were indeed useful shifts in critical pH with changes in chain configuration.[1] But the preparation of these samples required the use of a variety of polymerization methods, and variations in tacticity were accompanied by large differences in polymer molecular weight. Furthermore, the cooperativity of the conformational transition should be molecular weight dependent, so that the shape of the polymer-driven vesicle-to-micelle transition might be subject to control. We describe herein an investigation of the effects of polymer molecular weight on the structural reorganization of phosphatidylcholine vesicle membranes by poly(2-ethylacrylic acid).

Table I
Radical Polymerization of 2-Ethylacrylic Acid

sample	[AIBN], mol %	temp, °C	time, h	conv, %	$\bar{M}_w$	$\bar{M}_n$	$\bar{M}_w/\bar{M}_n$
P164	0.05	50	96	22	164 000	84 000	1.96
P43	0.50	60	22	24	43 000	22 000	1.96
P12	5.00	70	4.75	25	12 000	6 500	1.85

Experimental Section

Materials. Diethyl ethylmalonate, formaldehyde solution (37% w/w in water), diethylamine, and pyrene were obtained from Aldrich Chemical Co. and used without further purification. Azobis(isobutyronitrile) (AIBN) was purchased from Aldrich and recrystallized from methanol. Synthetic L-α-dipalmitoylphosphatidylcholine (approximately 99%) was obtained from Sigma Chemical Co. and used without further purification. Cellulose dialysis tubing (Spectra/Por 6, molecular weight cutoff 1000) was purchased from Fisher Scientific Co.

Polymerization. 2-Ethylacrylic acid (EAA) was synthesized from diethyl ethylmalonate by the method described earlier.[9] The monomer was distilled twice (bp = 48 °C (0.8 mm Hg)) and transferred to ampules [10 g (0.1 mol) per ampule]. After adding AIBN each reaction mixture was degassed by three freeze–thaw cycles and each ampule was sealed under vacuum. Various polymerization temperatures and AIBN concentrations were chosen (cf. Table I) in order to obtain samples of different molecular weights. The reaction mixtures were then diluted with diethyl ether and filtered, and the recovered polymer was washed with ether and dried under vacuum. In order to remove residual monomer the polymer samples were suspended in water and

0024-9297/89/2222-0765$01.50/0